frontiers | Frontiers in Carbon

TYPE Original Research
PUBLISHED 02 February 2024
DOI 10.3389/frcrb.2024.1352122

OPEN ACCESS

EDITED BY
Anthony B. Dichiara,
University of Washington, United States

REVIEWED BY
Chi-Hsien Huang,
Ming Chi University of Technology, Taiwan
Octavian Buiu,
National R&D Institute for Microtechnologies-IMT Bucharest, Romania

*CORRESPONDENCE
Matheus F. F. das Neves,
matheusfneves@gmail.com
Lucimara S. Roman,
lucimara.roman@ufpr.br

RECEIVED 07 December 2023
ACCEPTED 17 January 2024
PUBLISHED 02 February 2024

CITATION
das Neves MFF, Mukim S, Ferreira MS and Roman LS (2024), Mechanisms of methanol detection in graphene oxide and conductive polymer active layers for gas sensing devices. *Front. Carbon* 3:1352122.
doi: 10.3389/frcrb.2024.1352122

Mechanisms of methanol detection in graphene oxide and conductive polymer active layers for gas sensing devices

Matheus F. F. das Neves[1]*, Shardul Mukim[2], Mauro S. Ferreira[2,3] and Lucimara S. Roman[1]*

[1]Department of Physics, Federal University of Paraná, Curitiba, Paraná, Brazil, [2]School of Physics, Trinity College Dublin, Dublin, Ireland, [3]Centre for Research on Adaptive Nanostructures and Nanodevices (CRANN) and Advanced Materials and Bioengineering Research (AMBER) Centre, Trinity College Dublin, Dublin, Ireland

The admixture of PEDOT:PSS with Graphene Oxide (GO) in precise proportions achieves a substantial reduction in electrical resistivity, thereby augmenting its suitability as an electrode in organic devices. This study explores the electrical and morphological attributes of commercial PEDOT:PSS and chemically synthesized aqueous PEDOT ink when both are combined with GO. The investigation extends to the application of these conductive inks as active layers in flexible methanol sensing devices. Notably, a resistivity minimum is observed in the case of GO: PEDOT:PSS 78%, while the highest response to methanol is attained with GO: PEDOT:PSS 68%. To establish a theoretical underpinning for these findings, and to understand the interaction between gas/vapors with nanostructured materials, a model rooted in Kirchhoff's Circuit approach is developed, with the aim of elucidating the factors behind the resistivity minimum and response maximum at distinct specific mass ratios between PEDOT and GO. Calculating the equivalent resistivity and response of the systems, the positions of minimum and maximum points are in agreement with the experimental data. Furthermore, the influence of PSS in the samples is examined, unveiling diverse interaction mechanisms between methanol molecules and the active layer, resulting in varying signals during the exposure to alcoholic vapor. The theoretical model is subsequently applied to these systems, demonstrating qualitative and quantitative agreement with the experimental results.

KEYWORDS

PEDOT, graphene oxide, gas sensor, nodal analysis, organic electronics

1 Introduction

Poly (3,4-ethylenedioxythiophene), commonly referred to as PEDOT, stands out as one of the most widely utilized conductive polymers in the realm of organic electronics. Its prevalence owes itself to its inherent attributes of high electrical conductivity, partial transparency and flexibility Anand et al. (2021); das Neves et al. (2019); Nie et al. (2023). However, the hydrophobic nature of this polymer necessitates its processing in polar solvents, including water. This requirement leads to the blending of PEDOT with soluble molecules and necessitates the use of additional additives to stabilize dispersion. Notably, the most prevalent combination involves polystyrene sulfonate, denoted as PSS, resulting in the composite PEDOT:PSS. The addition of an excess of PSS serves to increase the PEDOT

concentration in water, facilitating dispersion and enabling the commercialization of conductive inks in varying concentrations. Numerous studies in the literature highlight the utility of PEDOT:PSS in the domain of organic electronic devices.

In the context of Organic Photovoltaics (OPVs), PEDOT:PSS has found application both as a semi-transparent electrode Lee et al. (2020) and as a hole transport layer Miranda et al. (2021); Chang et al. (2023); de Jesus Bassi et al. (2021). This polymeric conductive ink has also found relevance in other devices, including batteries del Olmo et al. (2022), supercapacitors Yoonessi et al. (2019), and Organic Light Emitting Diodes (OLED) Cinquino et al. (2022); Gu et al. (2019). Moreover, in organic gas sensing devices, this material serves as an active layer, enabling interactions with specific gases or vapors. For instance, Pasupuleti et al. (2021) have proposed the combination of these materials to detect Nitrogen Dioxide (NO_2). Similarly, Alves et al. (2022) have demonstrated the use of PEDOT:PSS and graphene oxide for monitoring methanol in confined spaces and, unlike the present study, it showed how a nanostructuring process affects the devices' efficiency.

Particularly in recent years, advancements in deposition techniques have allowed for the fabrication of flexible devices. Conductive polymers and their derivatives play a pivotal role in this regard, as their application as inks enables deposition methods such as casting, spin coating, and slot-die coating. The inherent flexibility of these materials facilitates large-scale production through techniques like roll-to-roll, an industrial method that demands robust and flexible substrates. Consequently, these devices exhibit eco-friendliness and versatility, thanks to their plastic properties, lightweight nature, processability, and recyclability Carneiro et al. (2023). These properties motivates the use of acetate as a flexible substrate for sensor fabrication in this study.

Despite the advantages that PSS imparts in terms of water dispersibility and ink stabilization, it's important to note that PSS is an insulating polymer that can potentially compromise the full electrical properties of PEDOT. Numerous studies have demonstrated that additional treatments can significantly enhance electrical conductivity, often by orders of magnitude. One common approach involves the incorporation of carbon nano-materials, such as Graphene Oxide (GO). For instance, Borges et al. (2019) have shown that there exists an optimal mass ratio between GO and PEDOT where conductivity improves significantly, attributed to chain polymer alignment and additional doping facilitated by GO. Another strategy to augment PEDOT properties involves the use of polar solvents to remove PSS from samples, thereby improving the organization of polymeric films das Neves et al. (2019).

So it would be interesting to propose new fabrication routes that do not require further treatments. PEDOT, being inherently hydrophobic, presents challenges in achieving water dispersibility, although not insurmountable ones. das Neves et al. (2021) have demonstrated the production of substantial quantities of PEDOT aqueous dispersion through monomer polymerization in acetonitrile, employing Iron (III) chloride without additional surfactants or insulating polymers, and utilizing Cl^- as a counter-ion. This opens up the possibility of producing a PEDOT conductive ink without the need for PSS and the subsequent steps required to remove the insulating polymer. In this study, it is replicated an established method for polymerizing PEDOT aqueous conductive ink das Neves et al. (2021) and introduce a novel approach that substitutes GO for PSS, investigating the effect of PSS in PEDOT-based samples.

The developed conductive inks composed of PEDOT and GO are applied in this study as active layers for flexible devices to monitor alcohol in a confined set up environment. Furthermore, this study reveals the interaction differences between active layers using PSS (commercial inks) and without this insulating polymer (polymerized samples). The methanol sensor devices employed in this study rely on an active layer that adsorbs chemical species, yielding a real-time amplified electrical response. A significant advantage of organic sensing devices lies in their operation at room temperature, in contrast to inorganic counterparts, which often require much higher temperatures exceeding 100°C Alves et al. (2022); Afzal (2019). The use of room temperature devices holds particular appeal, especially in confined space environments, as it demands less energy and reduces the risk of accidents, and the sensors presented in this study are characterized at 21°C.

Many contaminants in such environments consist of volatile compounds, and these can be effectively detected using composites like PEDOT-based thin films Vigna et al. (2021); Fujita et al. (2022). GO dispersions can enhance these composites' electrical conductivity das Neves et al. (2019), transconductance, and response by increasing surface area and organizing polymer chains Alves et al. (2022). Alcoholic vapors such as methanol are frequently encountered in confined spaces like grain silos and fuel tanks Alves et al. (2022); Wu et al. (2022) and the presence of this toxic and flammable compound at specific concentrations or during extended exposures poses hazards to human health Hashemi et al. (2022).

This paper aims to investigate the interaction between alcoholic vapors and nanostructured materials, as the response varies depending on the constituents of the active layer. Additionally, the impact of PSS in the inks is examined by comparing commercial PEDOT:PSS with chemically synthesized PEDOT and their blends with GO. These thin films find application in organic and flexible sensor devices designed for monitoring methanol levels in confined spaces. This exploration provides a deeper understanding of the roles played by PSS and GO as dopants for PEDOT, both from experimental and theoretical perspectives.

2 Methodology

2.1 Materials

A commercial aqueous solution of PEDOT:PSS was procured from Sigma-Aldrich with a concentration of 1.3 wt% of polymer in water, containing 500 μg L^{-1} of PEDOT and 800 μg L^{-1} of PSS. Graphite was obtained from Nacional de Grafite (Graflake 99580, 99.8% carbon). Additionally, 3,4-ethylenedioxythiophene (EDOT) (99%), acetonitrile (HPLC, 99%), and anhydrous iron (III) chloride ($FeCl_3$, 97%) were sourced from Sigma-Aldrich. Deionized water (18 MΩ) was obtained using Elga Purelab Flex equipment. Flexible substrates were produced from conventional acetate transparency sheets.

2.2 Preparation of PEDOT, GO: PEDOT and GO: PEDOT: PSS

The PEDOT aqueous dispersion was obtained through the oxidative polymerization of EDOT using $FeCl_3$ in acetonitrile, followed by a series of washing steps with acetonitrile and deionized water, as detailed in das Neves et al. (2021). Additional information regarding the synthesis of PEDOT can be found in the Supplementary Information. An aqueous PEDOT ink was prepared by isolating the wet solid from the aforementioned synthesis procedure described in the Supplementary Information. Specifically, 1.25 g of wet solid PEDOT was placed in a 100 mL round-bottom glass flask, along with 50 mL of deionized water, and subjected to 1 h of bath sonication, with cooling facilitated by the addition of small ice portions. The GO aqueous dispersion was generated through the oxidation of graphite, followed by liquid exfoliation and centrifugation, ultimately resulting in the desired graphene oxide dispersion. The graphite oxidation procedure was carried out following Hummers' modified method established in the literature Mehl et al. (2014). Further details regarding the preparation of the GO aqueous dispersion can be found in the Supplementary Information. Additional information regarding the properties of GO can be found in the cited literature Mehl et al. (2014); Borges et al. (2019); das Neves et al. (2019).

To create the GO:PEDOT aqueous dispersion, 1.25 g of wet polymerized solid PEDOT was combined with 37 mL of GO aqueous dispersion (0.05 mg mL^{-1}) and 13 mL of deionized water in a 100 mL round-bottom glass flask. The mixture was subjected to 1 h of ultrasound bath sonication, with cooling aided by small ice portions. Following ultrasound sonication, the PEDOT and GO: PEDOT inks were stored in glass vials.

The GO:PEDOT:PSS conductive inks were formulated by adding varying volumes (30, 60, 90, 120, 150, and 300 μL) of commercial PEDOT:PSS to 3 mL of GO aqueous dispersion. The mixture underwent 24 h of vigorous magnetic stirring, as previously described in Borges et al. (2019); das Neves et al. (2019); Holakoei et al. (2020). These samples were denoted as GO:PEDOT:PSS, followed by the respective percentage, corresponding to the concentration of PEDOT relative to GO. This concentration was calculated based on the molar mass and mass ratio established in prior studies, resulting in the following percentages: GO:PEDOT: PSS 40%, 59%, 68%, 74%, 78%, and 88%. The 100% sample represents pure PEDOT:PSS. Notably, GO:PEDOT:PSS 78% exhibits a mass ratio of 5.8×10^{-2} of GO/PEDOT, which is reported as the optimal proportion concerning electrical conductivity and optical transmittance on glass substrates Borges et al. (2019); das Neves et al. (2019).

2.3 Preparation of substrates and deposition of thin films

Interdigitated electrodes were meticulously prepared on commercial flexible acetate substrates using standard photolithography techniques, following the methodology outlined in Eising et al. (2017); Alves et al. (2022). These electrodes consisted of sputtered chromium followed by gold thin films, featuring an active area of 10 mm^2 and a band spacing of 100 μm. The configuration of the interdigitated electrodes is visually depicted in Figure 1. Electrical contacts were securely attached to the electrodes using silver conductive epoxy adhesive (model 8331S-14G by MG Chemicals) and subsequently dried on a hot plate at 65°C for a duration of 3 h.

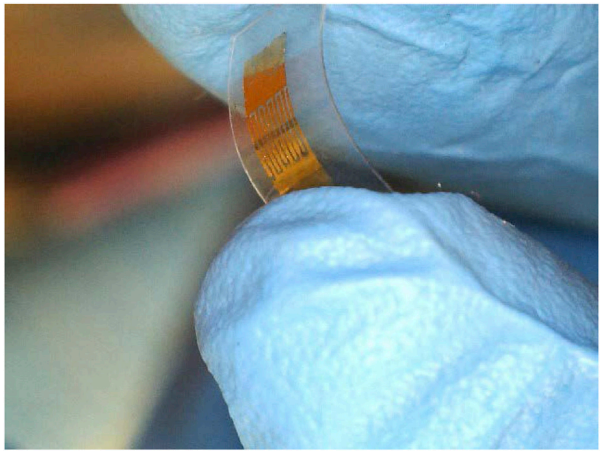

FIGURE 1
Interdigitated electrode in acetate, prepared using photolithography, to be used as substrate for the sensing device.

To create various gas sensors, a drop-casting approach was employed, depositing 10 μL of PEDOT, GO:PEDOT, GO:PEDOT: PSS, and neat PEDOT:PSS on the electrodes. The deposited thin films were left to dry at room temperature for a period of 24 h. Following the drying process, the thin films underwent thermal annealing at 40°C, utilizing a heating plate (IKA, model C-MAG HS 7), for 5 min. All of these procedures were carried out under standard room atmospheric conditions.

For thin films intended for morphological and electrical characterization, the same steps were followed. However, these films were deposited on 1 cm^2 acetate substrates without interdigitated electrodes.

2.4 Samples and sensors characterization

Morphological characterization was conducted utilizing Scanning Electron Microscopy (SEM) images, acquired with a TESCAN MIRA 3 FEG-SEM microscope operating at 10 kV and a working distance of 5 mm. Stubs with carbon paper were employed, ensuring electrical contact through copper adhesive ribbon.

Sheet resistance values were determined through four-probe measurements performed on acetate substrates utilizing Jandel Universal probe equipment. For each sample, these measurements were carried out 10 times, employing both forward and reverse electrical currents bias for each measurement. Subsequently, electrical conductivity was calculated using the relation $\sigma = \frac{1}{R_s \times t}$, where R_s represents the sheet resistance, and t denotes the thickness of the thin films. Thickness values were obtained through profilometry using a Veeco Dektak 150 instrument.

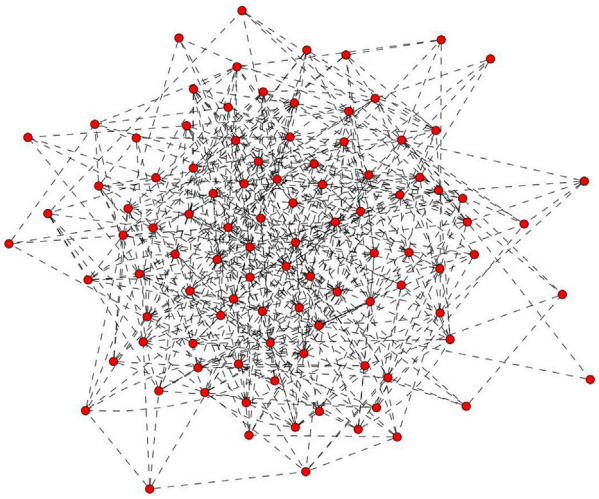

FIGURE 2
Random network (RNW) to depict a GO:PEDOT:PSS system.

Dynamic Light Scattering (DLS) measurements were conducted using a Malvern Zetasizer Nano Zs, model ZEN 3600, operating at 25°C with a 633 nm laser. A total of 20 measurements were performed for 10 s each, with an equilibrium time of 30 s. Particle sizes were calculated using the Mark-Houwink model. Zeta potential was determined using a Malvern Zetasizer Nano S at 25°C, involving 3 measurements for each sample, with 20 acquisitions each and an equilibrium time of 30 s.

The sensor response, represented as the change in electrical resistance, was characterized by calculating the absolute value of the difference between the electrical resistance of the device when exposed to the analyzed gas (R) and the electrical resistance under dry air conditions (R0). This value was then divided by R0 and presented as a percentage. To assess the response of the sensors to methanol (CH_3OH) in dry air, a setup consisting of a sensor probe within a tubular system was employed. Gas intake was controlled using a flowmeter and solenoid valves, as previously described in other studies Eising et al. (2017); Alves et al. (2022). All sensors were tested five times over a span of 2 weeks. The established methanol concentration was maintained at 1,000 ppm.

Using a multimeter (Agilent 34401A), the electrical resistance of the device and its changes during gas flow were continuously monitored in a controlled environment with 0% air humidity and a temperature of 21°C. The set up maintains air humidity through rotameters and dry air flowing through sample environment, while room temperature is controlled by an air conditioner and monitored using an LM35 connected to the system. Previous studies showed that 21°C is the optimum temperature that these sensors present a higher response. The same for air humidity, where if water is present, it can hinder methanol influence by swelling effect Alves et al. (2022). The samples were subjected to cycles of dry air for 3 min, followed by air containing the defined methanol concentration for 2 min. The device's measurements and gas intake were simultaneously controlled using a non-commercial software application.

2.5 Theoretical approach

There are very few theoretical descriptions based on real-world networks in which their physical characteristics are accounted for. Figure 2 depicts an example of a random network that resembles the connectivity of the PEDOT:PSS system. The problem of modelling such systems begins with the lack of information one can derive about connectivity. Most of these techniques are computationally very demanding as the physical characteristics depend on not just connectivity but material properties, and density to say a few.

O'Callaghan et al. (2016) showed that an effective medium approach provides a simple, but equivalent, way to evaluate properties of disordered networks with the help of an ordered square lattice network. In this study, it is considered a square lattice of dimensions 100 × 100. Every node is labeled as GO, PEDOT or PSS, and the weight of links, *i.e.*, resistance encodes the interactions between those constituents.

The equivalent resistance between the two points on the network can be calculated as Eq. 1

$$R_{x,y} = \left(M^{-1}_{x,x} + M^{-1}_{y,y} - M^{-1}_{x,y} - M^{-1}_{y,x}\right) \quad (1)$$

Here, $R_{x,y}$ is the equivalent resistance between the electrodes placed at site x and y. M is Kirchoff's matrix that encodes the connectivity and interaction between the entities contributing to electronic transport.

To begin with, it is considered a system where each node was assigned to be GO, and as a result, all the links present in the network are identical to one another. Due to the insulating behavior of the Graphene Oxide the resistivity of such system is high. Adding PEDOT and/or PSS to the network reduces the concentration of GO nodes as it is introduced low-resistance links in the system. The resistivity associated with a purely GO network is significantly higher than the PEDOT:PSS doped system. As the concentration of PEDOT:PSS increases the resistivity of the network drops due to the highly conductive PEDOT-GO behavior. The addition of PEDOT:PSS to the GO system creates a competition of resistances that dominates the equivalent resistivity of the network. A minimum is identified when the resistance distribution of both GO and PEDOT dominates the equivalent resistance. This perfectly resembles the resistivity minimum position determined in the experiments.

The simplicity of the model facilitates the integration of methanol for assessing the sensing behavior. Interaction with methanol can be modeled in the form of changes in the resistance of the links between neighboring nodes. The specific values assigned to each link are based on experimental data, reflecting the differences in resistance during exposure to methanol.

3 Results and discussions

3.1 Optimized samples—resistivity and response

The conductive inks containing commercial PEDOT:PSS were prepared by incorporating varying amounts of the polymeric compound into an aqueous Graphene Oxide (GO) dispersion.

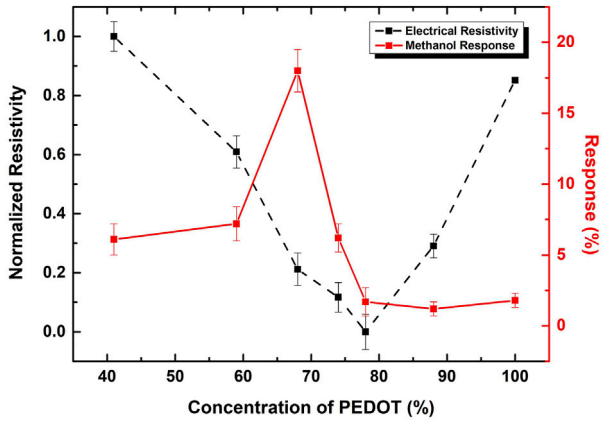

FIGURE 3
Black and dashed line shows the normalized resistivity values and Red and straight line shows the sensor response, both for GO:PEDOT: PSS 40, 59, 68, 74, 78, 88% and neat PEDOT:PSS deposited on acetate substrates. The response values corresponds to flexible sensor devices fabricated on interdigitated electrodes on top of acetate substrates.

The resulting materials were deposited on flexible acetate substrates for subsequent electrical and morphological characterization.

Previous studies have established that achieving a specific mass ratio of 5.8×10^{-2} between GO and PEDOT:PSS results in a minimum electrical resistivity. While this material has been used in Organic Photovoltaics Lima et al. (2016), the behavior was initially explored by Borges et al. (2019). They found that the sample with this precise mass ratio exhibited improved orientation of the thiophene groups within the PEDOT structure compared to lower and higher concentrations of PEDOT:PSS. This observation partially elucidates why the addition of a small amount of PEDOT:PSS to a GO aqueous dispersion, which inherently possesses insulator properties, leads to a more conductive compound than the conductor itself.

Figure 3 illustrates the normalized electrical resistivity values, represented by the black-dashed line, calculated using the sheet resistance, obtained from four-probe measurement, and the thicknesses of the thin films, that are around 250 nm. The results indicate that the lowest electrical resistivity is achieved with GO: PEDOT:PSS 78%. This concentration corresponds to the previously mentioned sample in the literature that aligns with the assigned mass ratio.

das Neves et al. (2019) conducted a study characterizing this optimized compound, investigating its morphological, optical, and electrical properties. In their research, they introduced a treatment that selectively removed a controlled amount of PSS, resulting in a more conductive thin film. Furthermore, both studies delved into charge transfer times, employing Resonant Auger Spectroscopy. Remarkably, the same sample that exhibited the minimum electrical resistivity also displayed a significantly reduced charge transfer time, determined using the Core Hole Clock method. This consistency aligns with the electrical measurements, reinforcing the pattern seen in the optimized sample.

The present study includes an additional characterization by replicating the ethyleneglycol treatment developed by das Neves and coauthors das Neves et al. (2019). The treatment involves dip-casting the dried thin films in ethyleneglycol followed by water, effectively removing PSS. Interestingly, the treatment reaffirmed that the minimum concentration remains consistent at GO:PEDOT: PSS 78%, as depicted in Supplementary Figure S1. The persistent occurrence of the minimum concentration is a topic of investigation in this present study and will be further discussed using the theoretical approach.

Methanol devices were fabricated using the interdigitated electrodes described in the experimental section. The electrode surfaces were coated by depositing 10 μL of each conductive ink, which included PEDOT, GO:PEDOT, PEDOT:PSS, and GO: PEDOT:PSS, with varying ratios between the components. In brief, the monitoring process commenced after the active layer was dried, and the devices were exposed to a controlled flow of the monitored vapor, all while maintaining a constant electrical current of 1 mA. The response was then determined by analyzing the variation in electrical resistance over time.

In the study conducted Alves et al. (2022), it was reported that the most favorable response to methanol vapor occurred with a mass ratio of 68% for GO:PEDOT:PSS, even though the highest electrical conductivity was observed at 78%. These findings, derived from sensors fabricated on glass substrates, aimed to explore a nanostructuring procedure to enhance sensing activity. In the current investigation, flexible methanol sensors are presented, employing the same method to produce GO:PEDOT:PSS inks, including the identical mass ratios previously published. The response rate results achieved with flexible devices, represented by the red-solid line in Figure 3, align with those reported by Alves et al. (2022). While there are slight variations in the response values compared to the previously cited study that employed the same inks, these differences, although less efficient, fall within the same order of magnitude. These variations can be attributed to the flexible nature of the devices, where surface interactions between the inks and the substrates contribute to differences in thin film morphology, including thickness and exposed active area. These factors directly influence the interaction between methanol and the active layers. Nonetheless, it is crucial to note that the qualitative behavior remains consistent.

The composite GO:PEDOT: PSS at a mass ratio of 68%, demonstrates the most favorable response, achieving a response of approximately 18%. Owing to this heightened response, subsequent experimental results involving GO and PEDOT:PSS will reference this specific percentage and the numerical value in the sample name will be omitted. Upon comparing the two curves, it becomes evident that beyond the concentration of 80%, the response remains independent of resistivity.

PEDOT:PSS represents an established commercial conductive ink that has found application in organic electronics for several decades. PEDOT, being hydrophobic, requires additives like stabilizers, surfactants, or negatively charged polyelectrolytes, such as PSS, to enable its dispersion in water. However, the electrical insulating properties of PSS can limit the full potential of PEDOT. Numerous published studies Lo et al. (2022); Saxena et al. (2019); Ouyang (2013) have explored the impact of PSS on PEDOT-based samples, highlighting its doping effect on PEDOT polymeric chains. Certain studies, such as the one conducted by das Neves et al. (2021), have introduced a synthesis route resulting in a

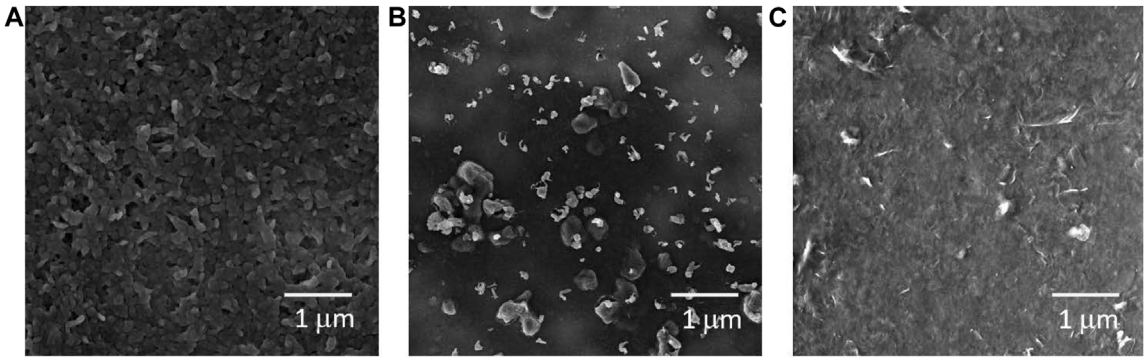

FIGURE 4
Scanning Electron Microscopy images for **(A)** PEDOT, **(B)** GO:PEDOT, and **(C)** GO:PEDOT:PSS 68% deposited on acetate substrates by drop casting.

pure PEDOT sample in water, utilizing electrostatic repulsion to stabilize the dispersion. This process yields electrical conductivity levels approaching that of commercial PEDOT:PSS. This study replicate both the aforementioned PEDOT synthesis route and introduce a new method incorporating GO. The aim is not only to compare morphology and electrical properties but also to investigate the mechanism of gas sensing devices. This comparison encompasses commercial PEDOT:PSS and the polymerized aqueous conductive ink PEDOT, both of which include GO in their composition.

3.2 Coloidal and morphological properties

GO:PEDOT samples exhibit an average particle size of approximately 480 nm, which is 300 nm larger than the reported size of PEDOT das Neves et al. (2021) and the DLS graph is depicted in Supplementary Figure S2. The ζ potential for this ink is +45.8 mV, indicating a metastable state, similar to the equilibrium state of the aqueous PEDOT ink. GO:PEDOT samples can be stored in glass flasks at low temperatures (4°C) for up to 4 months without coagulation, providing ample usability. The electrical resistivity of GO:PEDOT samples is approximately 0.35 Ωcm^{-1}, whereas for PEDOT samples, it stands at 0.45 Ωcm^{-1}. These resistivity values were calculated for samples with thicknesses of 290 nm and 230 nm, respectively. These results are within the same order of magnitude as previous characterizations presented in the literature for PEDOT aqueous ink deposited on glass substrates das Neves et al. (2021). Notably, the difference lies in the present study, where the thin films are deposited via drop casting on flexible acetate substrates. These electrical measurements indicate that the resistivity of the polymerized compounds remains competitive with the commercial PEDOT:PSS.

SEM images are displayed in Figure 4. Thin films of PEDOT (a) and GO:PEDOT:PSS 68% (c) exhibit homogeneity and even distribution on the substrates. In contrast, Figure 4B presents the GO:PEDOT sample, characterized by numerous clusters that may have formed during the polymerization process. These clusters appear to be comprised of GO sheets covered by a polymeric mass of PEDOT. These results align with previously published findings das Neves et al. (2021); Borges et al. (2019); das Neves et al. (2019); Alves et al. (2022). Figure 4A illustrates the polymeric mass of PEDOT nanoparticles, while Figure 4C highlights the polymeric appearance of the sample with exposed GO sheets spanning the substrate. Supplementary Figure S3 provides additional images for various concentrations of GO:PEDOT:PSS and includes PEDOT and GO:PEDOT comparison in a 500 nm scale.

3.3 Response over time

Figure 5 presents the percentage values, representing the sensor response, over time, comparing inks with and without PSS. The cycles denote exposure to methanol followed by dry air, each at a concentration of 1,000 ppm, complemented by additional cycles following the same pattern. In a previous study Alves et al. (2022) varied the methanol concentration from 1×10^3 to 450×10^3 ppm in order to calculate Freundlich Isotherm. It was concluded that GO:PEDOT:PSS exhibited a higher affinity than the commercial active layer, corroborating the reported results in this work. As expected, higher methanol concentrations presented higher response as the atmosphere is much more saturated. Moreover, it was demonstrated that below this minimum concentration, neat PEDOT:PSS active layer shows no response. Based on this prior characterization, the methanol concentration of 1,000 ppm was chosen to conduct the present analyzes.

The calculated percentage efficiency varies among the tested materials, with GO:PEDOT:PSS exhibiting the highest efficiency at 18%, followed by the PEDOT:PSS sample at around 4%, and both PEDOT and GO:PEDOT at approximately 2% and 1.5%, respectively. These results emphasize the increase in efficiency achieved by incorporating GO only in samples containing PSS, as previously predicted, reaffirming the necessity of this insulating component to enhance the doping effect by GO. This significant improvement can still be attributed to the larger surface area offered by GO sheets, facilitating enhanced adsorption of methanol molecules and, consequently, resulting in higher efficiency compared to active layers composed only of PEDOT:PSS or PEDOT.

Despite the presence of functional groups in GO, which may impede its electrical conductivity, several studies have demonstrated the interaction between PEDOT and GO, resulting in polymer chain

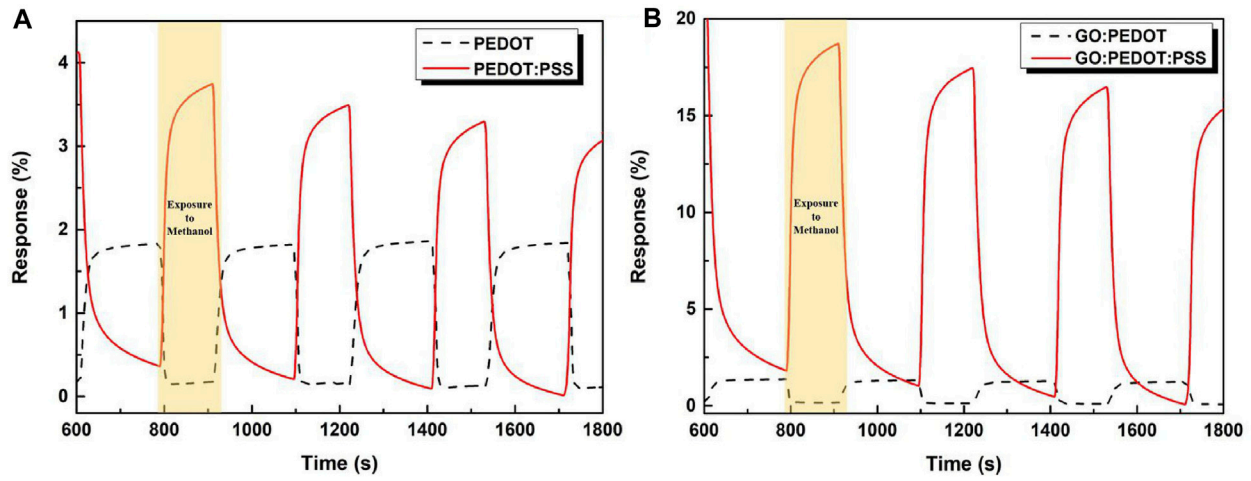

FIGURE 5
Response rate of the different devices in function of time and exposure to methanol for samples **(A)** Commercial ink PEDOT:PSS and chemically synthesized PEDOT and **(B)** Commercial ink PEDOT:PSS and chemically synthesized PEDOT, both with GO in its composition.

alignment and improved electrical conductivity Holakoei et al. (2020); das Neves et al. (2019); Borges et al. (2019); Alves et al. (2022). Additionally, these studies have revealed that GO effectively separates the PEDOT and PSS components, exposing PEDOT on the surface of the thin film. This exposure promotes a more intense interaction with methanol, consequently increasing sensor activity.

Furthermore, Alves et al. (2022) elucidated an additional doping effect engendered by the interaction between GO and PEDOT, facilitating the movement of more free charges that can interact with the monitored gas or vapor. An examination of SEM images reveals that the GO:PEDOT:PSS sample exposes GO sheets on the thin film's surface, correlating the heightened efficiency with the expanded surface area enabled by GO Hasani et al. (2015). Conversely, in GO:PEDOT samples, clusters of GO coated with PEDOT are observable. While GO:PEDOT exhibits a similar efficiency percentage when compared to polymerized samples, this can be attributed to the presence of clusters hinders even with the increased availability of charges. However, the response value does not approach that of GO:PEDOT:PSS due to inadequate cluster connectivity. Eising et al. (2021) demonstrated that cluster size and connectivity impact the response to exposed gas/vapor. In cases where clusters are large and well-connected, the electrical inner resistance increases while the electrical contact resistance decreases in relation to the contact area between clusters. The cluster sizes in this study are comparable; however, the distribution does not permit proper interconnection, resulting in a transduction mechanism reliant on the bulky polymeric mass. Consequently, the efficiency remains akin to that of a pure PEDOT sensor, despite the supplementary doping effect on the polymer chains.

Despite the superior performance of the commercial ink containing GO, it is noteworthy that, in the absence of GO, the polymerized PEDOT ink exhibits a comparable level of efficiency to that of the commercial PEDOT:PSS. The production of the polymerized aqueous PEDOT ink exclusively relies on water as a solvent, eliminating the need for stabilizers and surfactants. This characteristic not only enhances its ecological appeal but also contributes significantly to reduce production costs das Neves et al. (2021). Furthermore, the sensors manufactured using the internally produced PEDOT exhibit enhanced stability compared to their commercial counterparts, with faster saturation times. This stability is evident in the absence of any observable drift in the resistance curves. The efficiency values of active layers using the commercial polymers slightly drops over time in addition to the observed drift aspect. Eising et al. (2021) observed the same behavior for polyaniline and carbon nanotubes and suggested that it can be associated to local heating due to the current flow during the measurement procedure. Since PSS presents insulator properties, this effect can be pronounced in the samples containing this polymer.

Furthermore, it is worth noting that in the case of commercial samples containing PSS, their resistance increases upon exposure to methanol. Conversely, for the polymerized samples without PSS, the resistance decreases during exposure. This contrasting behavior can be attributed to various factors, including the swelling effect observed in samples containing PSS. Polar solvents like methanol and water can infiltrate the active layer due to interactions with PSS, which is a hygroscopic material. This infiltration leads to a separation of the polymeric chains, resulting in reduced connectivity and electrical conductivity Zeng et al. (2010); Yoon and Khang (2016). Additionally, the consumption of free charges plays a crucial role due to the reduction in methanol molecules, which increases the resistance of the devices Alves et al. (2022). In opposite, the absence of PSS may mitigate the swelling effect, and the decrease in resistance can be associated with the reorganization of charges, facilitated by the polymer being in a doped and conductive state das Neves et al. (2021). These phenomena will be further examined through theoretical modeling.

3.4 Theoretical modeling

The systems incorporating a graphene oxide network along with PEDOT and PSS can be analyzed using a theoretical framework to elucidate the observed outcomes. In this investigation, a GO network

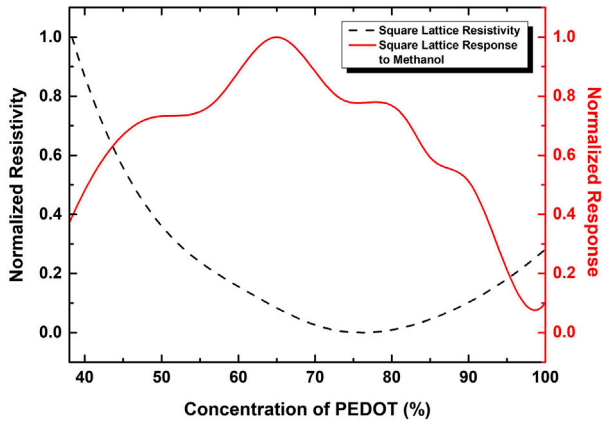

FIGURE 6
Normalized Resistivity values for the square lattice network representation of GO:PEDOT:PSS systems, indicated by the black-dashed line, showing the minimum in a determined concentration of PEDOT. Red-solid line represents the results for the Normalized Response Rate for methanol exposure, revealing the behaviour for different concentrations of PEDOT in GO network.

was employed to calculate the resistance or resistivity of the samples through the utilization of the Kirchoff matrix. The number of PEDOT and PSS entities was systematically altered to study their influence on the electrical properties of the network. It is important to note that the number of PEDOT and PSS components was maintained at the levels specified by the manufacturer, amounting to 0.5% for PEDOT and 0.8% for PSS, except when considering isolated PEDOT.

This simple model reveals the existence of an optimal concentration of PEDOT and GO, leading to the minimum resistivity. The graph in Figure 6 illustrates the outcomes obtained from a square lattice representation.

This result is consistent with the experimental data reported in this study and referenced in prior literature throughout the text. Despite the addition of PEDOT:PSS to the GO aqueous dispersion, and its corresponding lower volume fraction in the blend, the calculated ratios between the components, in terms of molar concentration, suggest that the optimal ratio is approximately 78% of PEDOT, a value remarkably close to the minimum value determined using the theoretical model, and it is showed by the black-dashed line.

The graph in Supplementary Figure S4 indicates a slightly different result for a random network. As expected, the minimum spot has changed to a lower value, approximately 65%, owing to the enhanced connectivity between the components compared to the square lattice. Nevertheless, these results are promising, considering the simplicity of this model and the proximity of the findings to those obtained with the square lattice representation, where connectivity is constrained to a maximum of 4.

These outcomes suggest a competition among the resistivities of the components within the network. Both GO and PSS are electrical insulators, with PEDOT being the conductive constituent in this blend. This competition in resistivities results in a global minimum. Prior to this optimal concentration, there isn't enough PEDOT to significantly enhance electrical conductivity, and both GO and PSS act as insulator pathways for charge carriers. Beyond this optimum concentration, the electrical conductivity of the sample approaches that of pure PEDOT. This conclusion aligns with the findings of Alves et al. (2022) and das Neves et al. (2019), where it is explicitly demonstrated that GO dopes PEDOT, increasing the number of free charges and, consequently, the electrical conductivity for this specific mass ratio. Furthermore, both sets of authors discuss the morphological changes induced by GO in the polymeric chains, contributing to improved electrical conductivity due to the synergistic effects of induced charge, polymer orientation, and morphology enhancement.

The identical network representation can also be employed to illustrate the sensor's response in the presence of methanol molecules. Figure 6 displays the response of the modeled sensors by the red-solid line, wherein the resistance links between the nodes are altered to signify methanol exposure, ensuring that the alcohol is distributed throughout every component, as per the saturated atmosphere during the experimental measurements.

The response reaches its maximum value at a concentration of approximately 65%, with both the Resistivity and Response curves following the pattern shown in Figure 3. It closely aligns with the performance of the GO:PEDOT:PSS 68% sample, and the findings are consistent with the research conducted by Alves et al. (2022). This behavior mirrors the pattern observed for the resistivity minimum. Despite both GO and PSS interact with methanol, the sensor's active layer must conduct the signal to the external circuit, and both GO and PSS are considered electrical insulators. PEDOT, being the conductive polymer, also interacts with the alcoholic vapor and efficiently carries the signals for monitoring. Alves et al. (2022) demonstrated that GO, by increasing the number of free charges, enhances the sensing activity, especially in specific concentrations. With a higher quantity of available charges, methanol molecules can consume these polarons, leading to an increase in the electrical resistance of the device and consequently enhancing the sensing activity.

Using this model improved to investigate the sensing activity, it was compared the samples with and without PSS. As depicted in Figure 5, when exposed to methanol molecules, the GO:PEDOT and PEDOT samples exhibit a decrease in electrical resistance, indicating sensor activity. However, in the presence of PSS within the system, the resistance increases, as indicated in both Figures 5A, B.

Alves et al. (2022) employed Density Functional Theory (DFT) to investigate the behavior of samples containing PSS when exposed to methanol. PSS is an insulating polymer often added to enhance the dispersibility of PEDOT in water while also doping PEDOT, increasing the number of empty states and facilitating hole mobility. However, polar molecules present in the surrounding atmosphere have the capacity to diminish this doping effect and, consequently, the electrical conductivity of the PEDOT chain.

In addition to these findings, the DFT data indicated a more pronounced doping effect when GO is introduced into the system, contributing to the increased efficiency with a favorable average adsorption energy. The authors suggested that GO enhances the availability of polarons. Consequently, the higher efficiency was attributed to GO:PEDOT:PSS samples due to the presence of GO, which amplifies the disruption of PEDOT doping caused by methanol molecules. Furthermore, the DFT results also revealed

interactions between GO, PEDOT, and PSS with methanol molecules through oxygenated groups. The mechanism, therefore, involves a process of PEDOT dedoping as a result of the consumption of available polarons by methanol molecules. In this case, methanol functions as a reducing agent, consistent with its chemical structure Saaedi et al. (2019); Singh and Sharma (2022).

In the current study, the application of the same model presented in the discussed results above is proposed. Supplementary Figure S5 illustrates the results for samples both with and without PSS. These findings demonstrate a qualitative alignment between the experimental data and the theoretical approach. While a comprehensive explanation for these results remains elusive and requires further investigation, certain observations can be made. Notably, the presence of PSS influences the resistance of the network. Both GO and PSS exhibit high electrical resistances, but PSS is an insulator polymer, whereas GO contains specific functional groups with insulating properties. Consequently, GO represents a component with high electrical resistance but also features regions that can conduct electricity, thereby engendering the desired interplay between resistances within the network, resulting in the observed contrasting behavior. Furthermore, the model posits that all components interact with methanol molecules, thereby giving rise to the step functions observed during exposure to the alcoholic vapor.

Methanol is recognized as a reducing agent, and changes in resistance within gas sensing devices are often associated with either doping or dedoping processes. Typically, an increase in resistance corresponds to a dedoping process, while a decrease implies doping. In this context, for methanol to reduce the electrical resistance, it should contribute charge carriers to PEDOT, effectively acting as an oxidizing agent. However, this is an unusual scenario, as it typically demands a substantial amount of energy to facilitate such a process. Additionally, catalytic reactions, which involve oxidizing agents for alcohols, do not apply in this case. Lin and Fan (2020) have discussed analogous behavior, where a decrease in resistance occurs in chemiresistive Carbon Dioxide (CO_2) gas sensors. In their study, CO_2 donates free electrons to the device, thereby increasing the number of free charges and subsequently enhancing electrical conductivity. Another aspect relevant to this specific case of charge flow in PEDOT samples relates to the redistribution of charges on the thin film's surface. The polymerized PEDOT in question exists in a doped state with polaron and bipolaron structures, as observed by das Neves et al. (2021). This rebalancing of charges can delocalize charge carriers and create new pathways, temporarily increasing the electrical conductivity of PEDOT samples. This reorganization results in the decrease of resistance during the exposure to methanol vapors instead of charge exchange as proposed for PEDOT:PSS-based samples.

4 Conclusion

This study investigated the utility of conductive inks composed of GO, PEDOT, and PEDOT:PSS, which were applied to flexible acetate substrates as active layers for methanol sensor devices. Electrical measurements revealed a minimum resistivity point corresponding to GO:PED-OT:PSS 78%, while the highest response to methanol, reaching up to 18%, was observed with GO:PEDOT:PSS 68%. Although the greatest values for both conductivity and response were associated with a commercial ink containing PSS, sensors crafted from the synthesized aqueous conductive ink consisting of pure PEDOT and GO:PEDOT demonstrated stability with sensitivities up to 2%. Furthermore, sensors with and without PSS exhibited different interaction mechanisms with the active layers. Flexible devices produced using commercial PEDOT:PSS experienced an increase in resistance upon exposure to methanol molecules, while pure PEDOT demonstrated a decrease in resistance values. Additionally, a model was developed to explore the aforementioned challenges, offering explanations for the global minimum in electrical resistivity and the maximum response. This approach employed a Kirchoff matrix within a square lattice representation and supported both qualitative and quantitative interpretations of the experimental data. The model illustrated the competition between the resistances of PEDOT, PSS, and GO, given that PEDOT is conductive while the latter two are insulators. Moreover, the model qualitatively represented the behavior of sensors with and without PSS, accounting for both resistance increase and decrease, respectively. This simple model effectively addressed the three research questions posed in this study, with the square lattice representation serving as a simplified yet powerful method for studying such systems, yielding results consistent with larger systems.

Data availability statement

The original contributions presented in the study are included in the article/Supplementary Material, further inquiries can be directed to the corresponding authors.

Author contributions

MdN: Conceptualization, Data curation, Investigation, Methodology, Writing–original draft, Writing–review and editing, Formal Analysis, Software. SM: Conceptualization, Formal Analysis, Methodology, Software, Writing–review and editing. MF: Conceptualization, Formal Analysis, Resources, Supervision, Validation, Writing–review and editing. LR: Formal Analysis, Funding acquisition, Methodology, Supervision, Writing–review and editing.

Funding

The author(s) declare financial support was received for the research, authorship, and/or publication of this article. MdN acknowledges CAPES—PRINT for the scholarship with process number 88887.694786/2022-00 and CNPq for the scholarship with process number 140712/2020-8.

Acknowledgments

The authors acknowledge CNPq, CAPES, Fundação Araucária and INCT Nanocarbono for funding. We thank Centro de Microscopia Eletrônica (CME) for SEM images. MdN thanks CNPq and CAPES—PRINT for the fellowship.

Conflict of interest

The authors declare that the research was conducted in the absence of any commercial or financial relationships that could be construed as a potential conflict of interest.

Publisher's note

All claims expressed in this article are solely those of the authors and do not necessarily represent those of their affiliated organizations, or those of the publisher, the editors and the reviewers. Any product that may be evaluated in this article, or claim that may be made by its manufacturer, is not guaranteed or endorsed by the publisher.

Supplementary material

The Supplementary Material for this article can be found online at: https://www.frontiersin.org/articles/10.3389/frcrb.2024.1352122/full#supplementary-material

References

Afzal, A. (2019). β-Ga2O3 nanowires and thin films for metal oxide semiconductor gas sensors: sensing mechanisms and performance enhancement strategies. *J. Materiomics* 5, 542–557. doi:10.1016/j.jmat.2019.08.003

Alves, L. S., Neves, M. F. F. d., Benatto, L., Ramos, M. K., Eising, M., de Oliveira, C. K. B., et al. (2023). Influence of nanostructuring sensors based on graphene oxide and pedot: pss for methanol detection. *IEEE Sensors J.* 23, 1845–1853. doi:10.1109/jsen.2022.3228954

Anand, A., Madalaimuthu, J. P., Schaal, M., Otto, F., Gruenewald, M., Alam, S., et al. (2021). Why organic electronic devices comprising pedot: pss electrodes should be fabricated on metal free substrates. *ACS Appl. Electron. Mater.* 3, 929–943. doi:10.1021/acsaelm.0c01043

Bassi, M. d. J., Wouk, L., Renzi, W., Oliveira, C. K., Duarte, J. L., Heisler, I. A., et al. (2021). Non-radiative energy transfer in aqueously dispersed polymeric nanoparticles for photovoltaic applications. *Synth. Met.* 275, 116740. doi:10.1016/j.synthmet.2021.116740

Borges, B. G. A. L., Holakoei, S., F das Neves, M. F., W de Menezes, L. C., de Matos, C. F., Zarbin, A. J., et al. (2019). Molecular orientation and femtosecond charge transfer dynamics in transparent and conductive electrodes based on graphene oxide and pedot: pss composites. *Phys. Chem. Chem. Phys.* 21, 736–743. doi:10.1039/c8cp05382k

Carneiro, M., das Neves, M. F., de Muniz, G. I., Filho, M. A. S. C., Oliveira, C. K., and Roman, L. S. (2023). Ecological, flexible and transparent cellulose-based substrates without post-production treatment for organic electronic devices. *J. Mater. Sci. Mater. Electron.* 34, 186–219. doi:10.1007/s10854-022-09667-8

Chang, Y.-M., Li, W.-L., Tsai, C.-H., and Teng, N.-W. (2023). Mitigating the efficiency loss of organic photovoltaic cells using phosphomolybdic acid-doped pedot: pss as hole transporting layer. *Adv. Energy Sustain. Res.* 4, 2300006. doi:10.1002/aesr.202300006

Cinquino, M., Prontera, C. T., Zizzari, A., Giuri, A., Pugliese, M., Giannuzzi, R., et al. (2022). Effect of surface tension and drying time on inkjet-printed pedot: pss for ito-free oled devices. *J. Sci. Adv. Mater. Devices* 7, 100394. doi:10.1016/j.jsamd.2021.09.001

das Neves, M. F., Damasceno, J. P. V., Junior, O. D., Zarbin, A. J., and Roman, L. S. (2021). Conductive ink based on pedot nanoparticles dispersed in water without organic solvents, passivant agents or metallic residues. *Synth. Met.* 272, 116657. doi:10.1016/j.synthmet.2020.116657

das Neves, M. F. F., Damasceno, J. P. V., Holakoei, S., Rocco, M. L. M., Zarbin, A. J. G., De Oliveira, C. K. B. Q. M., et al. (2019). Enhancement of conductivity and transmittance of graphene oxide/pedot: pss electrodes and the evaluation of charge transfer dynamics. *J. Appl. Phys.* 126, 215107. doi:10.1063/1.5124619

del Olmo, R., Mendes, T. C., Forsyth, M., and Casado, N. (2022). Mixed ionic and electronic conducting binders containing pedot: pss and organic ionic plastic crystals toward carbon-free solid-state battery cathodes. *J. Mater. Chem. A* 10, 19777–19786. doi:10.1039/d1ta09628a

Eising, M., Cava, C. E., Salvatierra, R. V., Zarbin, A. J. G., and Roman, L. S. (2017). Doping effect on self-assembled films of polyaniline and carbon nanotube applied as ammonia gas sensor. *Sensors Actuators B Chem.* 245, 25–33. doi:10.1016/j.snb.2017.01.132

Eising, M., O'Callaghan, C., Eduardo Cava, C., Schmidt, A., Gorgatti Zarbin, A. J., Ferreira, M. S., et al. (2021). The role of carbon nanotubes on the sensitivity of composites with polyaniline for ammonia sensors. *Carbon Trends* 3, 100026. doi:10.1016/j.cartre.2021.100026

Fujita, H., Hao, M., Takeoka, S., Miyahara, Y., Goda, T., and Fujie, T. (2022). Paper-based wearable ammonia gas sensor using organic–inorganic composite pedot: pss with iron (iii) compounds. *Adv. Mater. Technol.* 7, 2101486. doi:10.1002/admt.202101486

Gu, Z.-Z., Tian, Y., Geng, H.-Z., Rhen, D. S., Ethiraj, A. S., Zhang, X., et al. (2019). Highly conductive sandwich-structured cnt/pedot: pss/cnt transparent conductive films for oled electrodes. *Appl. Nanosci.* 9, 1971–1979. doi:10.1007/s13204-019-01006-4

Hasani, A., Dehsari, H. S., Gavgani, J. N., Shalamzari, E. K., Salehi, A., Afshar Taromi, F., et al. (2015). Sensor for volatile organic compounds using an interdigitated gold electrode modified with a nanocomposite made from poly (3, 4-ethylenedioxythiophene)-poly (styrenesulfonate) and ultra-large graphene oxide. *Microchim. Acta* 182, 1551–1559. doi:10.1007/s00604-015-1487-7

Hashemi, S. A., Bahrani, S., Mousavi, S. M., Omidifar, N., Arjmand, M., Lankarani, K. B., et al. (2022). Differentiable detection of ethanol/methanol in biological fluids using prompt graphene-based electrochemical nanosensor coupled with catalytic complex of nickel oxide/8-hydroxyquinoline. *Anal. Chim. Acta* 1194, 339407. doi:10.1016/j.aca.2021.339407

Holakoei, S., Veiga, A. G., Turci, C. C., das Neves, M. F. F., Wouk, L., V Damasceno, J. P., et al. (2020). Conformational and electron dynamics changes induced by cooling treatment on go: pedot: Pss transparent electrodes. *J. Phys. Chem. C* 124, 26640–26647. doi:10.1021/acs.jpcc.0c07827

Kim, D. H., Lee, D. J., Kim, B., Yun, C., and Kang, M. H. (2020). Tailoring pedot: pss polymer electrode for solution-processed inverted organic solar cells. *Solid-State Electron.* 169, 107808. doi:10.1016/j.sse.2020.107808

Lima, L., Matos, C., Gonçalves, L., Salvatierra, R., Cava, C., Zarbin, A., et al. (2016). Water based, solution-processable, transparent and flexible graphene oxide composite as electrodes in organic solar cell application. *J. Phys. D Appl. Phys.* 49, 105106. doi:10.1088/0022-3727/49/10/105106

Lin, Y., and Fan, Z. (2020). Compositing strategies to enhance the performance of chemiresistive co2 gas sensors. *Mater. Sci. Semicond. Process.* 107, 104820. doi:10.1016/j.mssp.2019.104820

Lo, C.-Y., Wu, Y., Awuyah, E., Meli, D., Nguyen, D. M., Wu, R., et al. (2022). Influence of the molecular weight and size distribution of pss on mixed ionic-electronic transport in pedot: pss. *Polym. Chem.* 13, 2764–2775. doi:10.1039/d2py00271j

Mehl, H., Matos, C. F., Neiva, E., Domingues, S., and Zarbin, A. (2014). The effect of variation of reactional parameters in the preparation of graphene by oxidation and reduction of graphite. *Quím. Nova* 37. doi:10.5935/0100-4042.20140252

Miranda, B. H., Corrêa, L. d. Q., Soares, G. A., Martins, J. L., Lopes, P. L., Vilela, M. L., et al. (2021). Efficient fully roll-to-roll coated encapsulated organic solar module for indoor applications. *Sol. Energy* 220, 343–353. doi:10.1016/j.solener.2021.03.025

Nie, S., Qin, F., Liu, Y., Qiu, C., Jin, Y., Wang, H., et al. (2023). High conductivity, semiconducting, and metallic pedot: pss electrode for all-plastic solar cells. *Molecules* 28, 2836. doi:10.3390/molecules28062836

O'Callaghan, C., Gomes da Rocha, C., Manning, H. G., Boland, J. J., and Ferreira, M. S. (2016). Effective medium theory for the conductivity of disordered metallic nanowire networks. *Phys. Chem. Chem. Phys.* 18, 27564–27571. doi:10.1039/c6cp05187a

Ouyang, J. (2013). "secondary doping" methods to significantly enhance the conductivity of pedot: pss for its application as transparent electrode of optoelectronic devices. *Displays* 34, 423–436. doi:10.1016/j.displa.2013.08.007

Pasupuleti, K. S., Reddeppa, M., Nam, D.-J., Bak, N.-H., Peta, K. R., Cho, H. D., et al. (2021). Boosting of no2 gas sensing performances using go-pedot: pss nanocomposite chemical interface coated on langasite-based surface acoustic wave sensor. *Sensors Actuators B Chem.* 344, 130267. doi:10.1016/j.snb.2021.130267

Saaedi, A., Shabani, P., and Yousefi, R. (2019). High performance of methanol gas sensing of zno/pani nanocomposites synthesized under different magnetic field. *J. Alloys Compd.* 802, 335–344. doi:10.1016/j.jallcom.2019.06.088

Saxena, N., Pretzl, B., Lamprecht, X., Bießmann, L., Yang, D., Li, N., et al. (2019). Ionic liquids as post-treatment agents for simultaneous improvement of seebeck coefficient and electrical conductivity in pedot: pss films. *ACS Appl. Mater. interfaces* 11, 8060–8071. doi:10.1021/acsami.8b21709

Singh, S., and Sharma, S. (2022). Temperature dependent selective detection of ethanol and methanol using mos2/tio2 composite. *Sensors Actuators B Chem.* 350, 130798. doi:10.1016/j.snb.2021.130798

Vigna, L., Verna, A., Marasso, S., Sangermano, M., D'Angelo, P., Pirri, F., et al. (2021). The effects of secondary doping on ink-jet printed pedot: pss gas sensors for vocs and no2 detection. *Sensors Actuators B Chem.* 345, 130381. doi:10.1016/j.snb.2021.130381

Wu, F., Pan, X., Wang, H., Hua, M., Yu, H., Zang, X., et al. (2022). Experimental study on the explosion characteristic and flame propagation of methanol spray at different injection pressures. *Fuel* 325, 124746. doi:10.1016/j.fuel.2022.124746

Yoon, S.-S., and Khang, D.-Y. (2016). Roles of nonionic surfactant additives in pedot: pss thin films. *J. Phys. Chem. C* 120, 29525–29532. doi:10.1021/acs.jpcc.6b12043

Yoonessi, M., Borenstein, A., El-Kady, M. F., Turner, C. L., Wang, H., Stieg, A. Z., et al. (2019). Hybrid transparent pedot: pss molybdenum oxide battery-like supercapacitors. *ACS Appl. Energy Mater.* 2, 4629–4639. doi:10.1021/acsaem.8b02258

Zeng, F.-W., Liu, X.-X., Diamond, D., and Lau, K. T. (2010). Humidity sensors based on polyaniline nanofibres. *Sensors Actuators B Chem.* 143, 530–534. doi:10.1016/j.snb.2009.09.050